

## Application of Optical Theory to Quantitative Surface FT-IR with Emphasis on Molecular Depth Profiling

Hatsuo ISHIDA\*

*Received March 24, 1993*

Applications of optical theory to the study of surface, thin films and coatings have been reviewed. Recent advances in personal computing has made the application of optical theory to an observed spectrum a nearly routine practice. With diversification of infrared techniques which rely on reflection techniques, band shape distortion and frequency shift are common occurrence and the ability to correct for the optical effects has become extremely useful. This article discusses selected topics to demonstrate the usefulness of the application of optical theory. Special emphasis is placed on the quantitative nature of the discussion as well as techniques related to molecular depth profiling.

KEY WORDS: Surface / Film / Coating / FT-IR / Reflection

### INTRODUCTION

Infrared spectroscopy (IR) is one of the oldest analytical techniques and has received a wide acceptance in analytical laboratories. A century-old technique enjoys an unmatched richness in a data base. In spite of its long history, infrared spectroscopy is still experiencing an active development of new approaches. Most notably is the development of surface IR spectroscopy in the past decade, which was made in part possible by the advent of Fourier transform infrared spectroscopy (FT-IR). Improved energy throughput, multiplex advantage and frequency accuracy allow previously impractical techniques by ordinary dispersive infrared spectrometers to be routinely performed. Today, there are IR techniques that can be applied for surface characterization for almost any form of sample. This remarkable diversification of IR techniques is summarized in Table 1 where variations of generic techniques along with their references (1-36) are also cited. More detailed description of surface FT-IR techniques can be found in a review article(37).

Diversification of IR techniques has made interpretation of IR spectra more complex and difficult. When transmission was the dominant choice of technique, the recorded spectra showed few artifacts due to optical perturbation. However, in recent years, reflection techniques are routinely used and spectral distortion became a daily occurrence. It should be recalled that an observed IR spectrum is a composite of the absorption properties and refractive indices whose contributions vary depending upon the technique, sample geometry, and optical configuration. Strong optical perturbation often leads to misinterpretation of spectra because of frequency shifts and relative intensity changes. An extreme case might show a

---

\*石田初男: Department of Macromolecular Science, Case Western Reserve University, Cleveland, Ohio 44106-7202, U.S.A.

Table 1. Various Infrared Spectroscopic Techniques that can be Used for Surface Characterization

Techniques	References
1. Transmission Spectroscopy	
1.1. Ordinary Transmission Spectroscopy	
1.2. Diffuse Transmission Spectroscopy	1
2. Reflection Spectroscopy	
2.1. Internal Reflection Spectroscopy	
2.1.1. Attenuated Total Reflection (ATR) Spectroscopy	
a. Ordinary ATR spectroscopy	2,3,4
b. Metal-overlayer ATR spectroscopy	5
c. Variable-angle ATR spectroscopy	6,7,8,9
2.2. External Reflection Spectroscopy	
2.2.1. Specular Reflection Spectroscopy	
a. Ordinary external reflection spectroscopy	
b. Reflection-absorption spectroscopy	10,11,12,13
c. Brewster-angle-incident external reflection spectroscopy	14
2.2.2. Diffuse Reflectance Spectroscopy	
a. Ordinary diffuse reflectance spectroscopy	15,16
b. KBr-overlayer diffuse reflectance spectroscopy	17,18
2.3. Surface Electromagnetic Wave (SEW) Spectroscopy	19,20,21,22
2.5. Infrared Ellipsometry	23,24,25,26
3. Emission Spectroscopy	
3.1. Ordinary Emission Spectroscopy	
3.2. Angularly-resolved Emission Spectroscopy	27,28,29
4. Photoacoustic Spectroscopy (PAS)	30,31,32,33
5. Photothermal Deflection Spectroscopy	34,35,36

band with a derivative appearance and a peak towards the negative of what is normally expected. While frequency shifts of  $20\text{ cm}^{-1}$  may be interpreted as a group with and without a hydrogen bond, it is not uncommon to observe frequency shifts of this magnitude simply by the optical perturbation in some configuration without any chemical reasons. Hence, it is indispensable in modern IR spectroscopy to incorporate interpretation based on the optical theory. This is especially important in reflection spectroscopy.

This paper describes selected techniques, often used for surface characterization, from a quantitative point of view wherever possible. Readers are referred to original papers for more detailed discussions. Emphasis is placed on the application of optical theory and molecular depth profiling. Application of optical theory to infrared spectra is not new. In fact, there exists a wealth of papers concerning optical theory in the literature dating back many decades. Nonetheless, it is only in the past decade that routine application of optical

theory became possible. Until recently, calculation of spectra had been tedious and application of the theory to daily spectral analysis was rarely routine. With the fast development of powerful personal computers in the past several years, spectral correction and interpretation based on the optical theory has become fairly straightforward in many laboratories. At present, the majority of spectral analyses based on the optical theory relies on software developed in individual laboratories; however, commercial programs are receiving attention and some are already available.

Along with the application of the optical theory and quantification of surface spectra, molecular depth profiling became possible. Some methods are still in their infancy and the depth information is at best qualitative. Others are understood more quantitatively but the depth information is resolved poorly. Yet, some have already shown promise to be useful in traditionally considered difficult resolution.

It should be emphasized that there are many depth profiling techniques with much better spatial resolutions available today. However, those are often the atomic techniques and molecular information is very difficult to obtain. There are techniques that provide information on molecular fragments, yet those techniques are not sensitive to minute structural changes. It is also common that those techniques are often destructive and require high vacuum. There is no assurance that true depth information in being probed rather than the induced structural information. Techniques described in this paper are non-destructive and some do not even require contact with the sample surface. Properties that can be studied as a function of the depth include, but not restricted to, chemical reactions, orientation, crystal structure and crystallinity, chain packing, conformation, configuration, and concentration. These are the properties which are very important in understanding adhesion of materials.

## EXPERIMENTAL

Any Fourier transform infrared spectroscopy can provide information described in this paper with some difference in degree of accuracy and signal-to-noise (S/N) ratio. The majority of the spectra shown in this paper were obtained by FT-IR spectrometers manufactured by Bomem (model DA-3 and Michelson-110) and Biorad (Digilab Model 20E). All spectrometers were purged with dry nitrogen gas and equipped with medium-band mercury-cadmium-telluride (MCT) detectors with specific detectivity,  $D^*$ , of  $1 \times 10^{10}$  cmHz<sup>0.5</sup>/W with the exception of Bomem DA-3 with  $D^* = 2.1 \times 10^{10}$  cmHz<sup>0.5</sup>/W. The DA-3 is evacuable to 0.1 torr and spectral collection was initiated when the vacuum reached at least 0.5 torr. All spectra shown in this paper were obtained at a resolution of 4 cm<sup>-1</sup> with varying number of scans but ranging from 50 to 2000 scans depending on the requirements of the S/N ratio.

Optical theory softwares were developed in-house using Fortran 77 available for VAX or micro-VAX (Digital) with VMS operating system. Detailed description of individual approaches has been reported elsewhere. In general, the program is based on the exact optical theory utilizing generalized matrix which allows many stratified layers to be studied without stringent assumptions. Agreement between theoretical calculation and experimentally obtained spectra is usually excellent, but its accuracy is strongly influenced by the accuracy of the spectrometer and attachment used. Optical constants, namely extinction coefficient,  $k$ ,

and refractive index,  $n$ , are all expressed as spectra rather than tabulated numbers.

### APPLICATION OF OPTICAL THEORY TO THIN FILM ANALYSES

Frequency shifts and intensity changes which are caused by the strong contribution of the refractive indices must be removed prior to spectral interpretation for chemical structural changes. Historically, infrared spectroscopy has been considered rather qualitative mainly due to the attempt to interpret spectra without correction by optical theory. In the application of optical theory to thin film analyses, there are two distinctively different approaches. The first, rather straight forward approach, is to calculate, from known refractive index spectrum,  $n$ , and extinction coefficient spectrum,  $k$ , a simulated spectrum for any particular optical configuration. To do this, in addition to the aforementioned optical constant spectra, angle of incidence, optical properties of prism and substrate materials if any, and thickness and number of layers of the thin film must be known. This approach is useful when evaluation of the optical distortion of a known material for a known configuration is desired. Conversely, when optical constants of an unknown material with often an unknown thickness are to be determined, a more rigorous approach must be taken. Once determination of optical constant spectra of the unknown sample is successful, the obtained spectra are intrinsic to the material property and independent of the material concentration or thickness and the optical configuration of the sampling attachment. Table 2 lists selected references for the above two approaches. References listed are not necessarily the first example in the literature since numerous old papers exist, but are the more recent examples that can be directly applied to the modern FT-IR spectroscopic configurations and softwares. Pioneering papers in each technique are cited in the references therein. Some papers concern calculation of intensity while others attempt to show spectrum as a function of frequency.

Of numerous examples of the application of optical theory, dramatic examples are shown below. A diffuse reflectance attachment can be used to obtain spectrum of powdery samples where strong scattering can be observed. Diffusely scattered radiation is collected while specularly reflected radiation is minimized by the arrangement of mirrors and use of a blocker. However, it is difficult to completely eliminate the specular component and diffuse reflectance spectrum is a composite of diffuse and specular components. Since specular component is not a part of Kubelka-Munk calculation which is most often used equation to analyze quantitatively the diffuse reflectance spectrum, specular component introduces non-linear dependence of the intensity to concentration. Spectral distortion is also observed especially for powders and fibers with low refractive indices. Such is the case where diffuse reflectance attachment is used to study polymeric fibers. Figure 1 compares the transmission spectrum of a thin film of poly(ethylene terephthalate) (PET) and the diffuse reflectance spectra of PET filaments. Since the fiber used was the sample prior to drawing process, no significant molecular orientation exists except that the shape of the sample is fibrous. Nonetheless, the difference in spectral characteristics is astounding due primarily to the optical effects. There are two classes of diffuse reflectance theory; one is continuum model such as the Kubelka-Munk theory and the other statistical model. In order to use physically meaningful quantities such as  $n$  and  $k$  spectra, statistical model must be used. An infinitesimally thin layer was presumed whose

Table 2. Papers related to the optical theory where simulation of infrared spectrum using optical constants or calculation of optical constants from observed infrared spectrum were mentioned.

Techniques	References	
	n, k to spectrum	spectrum to n, k
1. Transmission Spectroscopy		
1.1. Ordinary transmission Spectroscopy	38	39,40,41
2. Reflection Spectroscopy		
2.1. Internal Reflection Spectroscopy		
2.1.1. Attenuated Total Reflection (ATR) Spectroscopy		
a. Ordinary ATR spectroscopy	2	42,43,44,45,46
b. Metal-overlayer ATR spectroscopy	5	
c. Variable-angle ATR spectroscopy	8,9	
2.2. External Reflection Spectroscopy		
2.2.1. Specular Reflection Spectroscopy		
a. Ordinary external reflection spectroscopy	10,11	47,48,49
b. Reflection-absorption spectroscopy	14	50
c. Brewster-angle-incident external reflection spectroscopy	51	
2.2.2. Diffuse Reflectance Spectroscopy		
a. Ordinary diffuse reflectance spectroscopy	52	
2.4. Surface Electromagnetic Wave (SEW) Spectroscopy	21,22	
2.5. Infrared Ellipsometry	23,24,25,26	53
3. Emission Spectroscopy		
3.1. Ordinary Emission Spectroscopy	54,55,56	
3.2. Angularly-resolved Emission Spectroscopy	27,28,29	

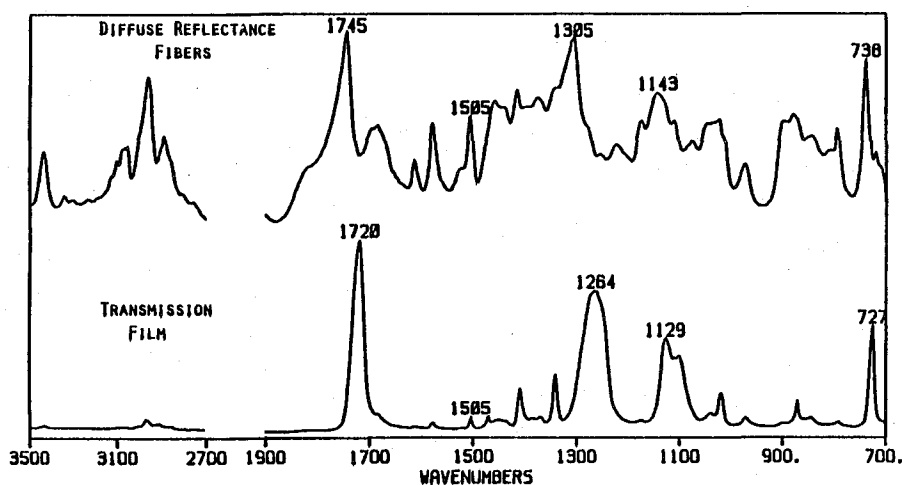


Figure 1. Comparison of a transmission spectrum of a solution cast PET film with a diffuse reflectance spectrum of undrawn PET fibers. Orientation of the PET molecules along the fiber axis is known to be minimal.

reflection and transmission is defined as  $r$  and  $t$ . For layers of these thin films, the following relationship exists (52).

$$R = \frac{1 + r^2 - t^2}{2r} - \sqrt{\left(\frac{1 + r^2 - t^2}{2r}\right)^2 - 1} \quad \text{Eq. [1]}$$

We assumed that many layers of thin films simulate an array of fibers and the infrared radiation must follow the above relationship. The simulated spectrum is compared in Figure

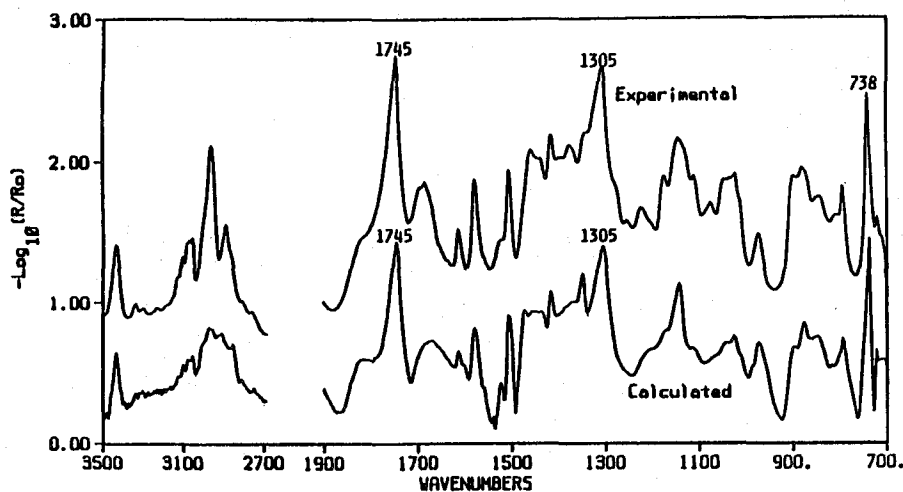


Figure 2. Comparison of experimentally observed diffuse reflectance spectrum of the undrawn PET fibers with spectrum calculated from equation 1 and optical constants determined from the transmission spectrum.

2 where excellent frequency agreement is obtained, in spite of quite substantial frequency mismatch of the initial transmission and reflection spectra. Some difference in intensity may come from the minor difference in conformation since the two samples used do not have exactly the same thermal history.

Another example is the simulation of ordered thin films such as Langmuir-Blodgett films on polymeric substrate (53). While amorphous materials are assumed to be three dimensionally homogeneous, ordered thin films possess different optical properties in the thickness direction ( $z$ ) as compared with the direction of the film length ( $x$ ) or width ( $y$ ). Usually,  $x$  and  $y$  directions are considered to possess the same optical properties. Thus, two sets of optical constants, known as ordinary optical constants and extraordinary optical constants, are needed to express the optical properties of an ordered thin film. The ordinary optical con-

stants are measured by the electric vector of an infrared radiation along the xy plane whereas the extraordinary optical constants are measured by the electric vector along the z direction. Experimentally, ordinary optical constants can be measured by transmission experiments through the thin or specular reflection with perpendicular polarization with respect to the plane of the incidence while extraordinary optical constants are measured by specular reflection with parallel polarization or infrared ellipsometry. Drude's equations for anisotropic films shown below were used to simulate the infrared spectrum of an LB film.

$$r_s = \frac{\cos \theta - (n_o^2 - \sin^2 \theta)^{1/2}}{\cos \theta + (n_o^2 - \sin^2 \theta)^{1/2}} \quad \text{Eq [2]}$$

$$r_p = \frac{n_e n_o \cos \theta - (n_e^2 - \sin^2 \theta)^{1/2}}{n_e n_o \cos \theta + (n_e^2 - \sin^2 \theta)^{1/2}} \quad \text{Eq [3]}$$

where  $n_o$  and  $n_e$  are ordinary and extraordinary optical constants and  $r_s$  and  $r_p$  are Fresnel coefficient of reflection with perpendicular and parallel polarizations, respectively. Figure 3

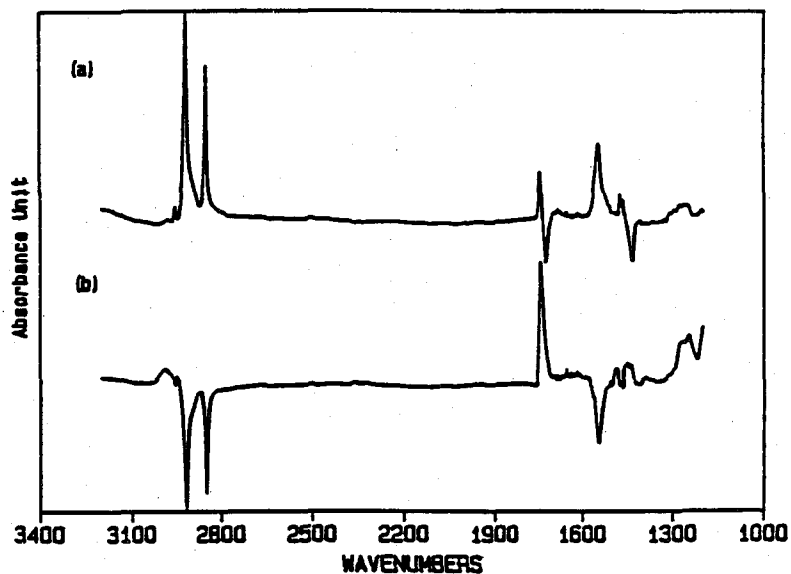


Figure 3. Experimental external reflection spectra of 40 layers of cadmium arachidate LB film on poly(methyl methacrylate) substrate at 75° using (a) parallel and (b) perpendicular polarized light.

shows the experimentally observed spectrum of a cadmium arachidate film on poly (methyl methacrylate) substrate. Note that in addition to ordinary band pointing upward, there are downward as well as derivative type bands. These band shapes and directions are solely caused by the optical reasons rather than chemical structures. A successful application of Drude's anisotropic equations to simulate the experimentally observed spectra shown above is an indication that an optical reason is the dominant factor for the unusual spectral appearance. Figure 4 illustrates simulated spectrum using two sets of optical constants and

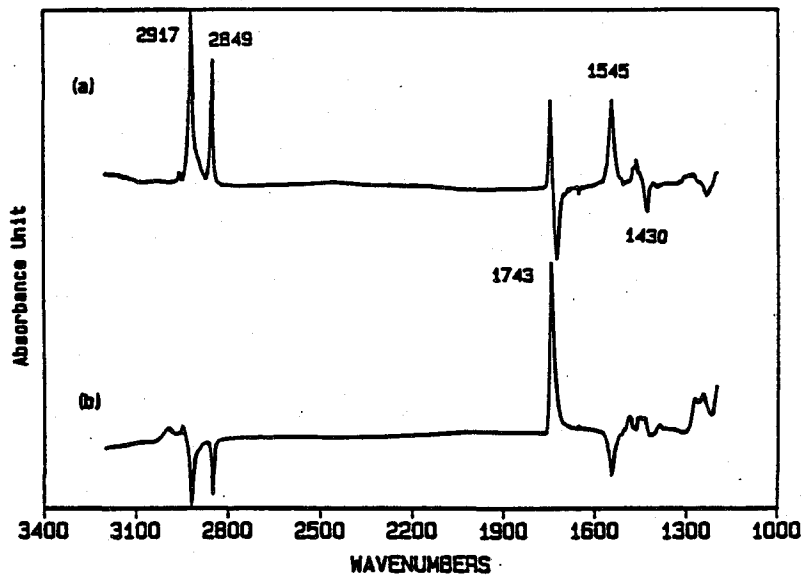


Figure 4. Simulated external reflection spectra under the same condition as in Figure 3. Ordinary and extraordinary optical constants were obtained by transmission and ellipsometric techniques, respectively.

Drude's equations for anisotropic media. A fairly good agreement between experimental and theoretical calculation has been obtained.

#### MOLECULAR DEPTH PROFILING

There are several techniques which are suitable for depth profiling. For example, photoacoustic spectroscopy allows depth profiling to be done on the order of several tens micrometers by changing the modulation frequency, in other word, the speed of the scanning mirror in FT-IR spectrometer. The depth,  $l_{\beta}$ , at which initial infrared intensity,  $I_0$ , attenuates to  $(1/e)I_0$ , is expressed as  $l_{\beta} = (2\alpha_S/\omega)^{1/2}$ , where  $\alpha_S$  is the thermal diffusivity of the sample. As the modulation frequency increases, the probing depth decreases. However, the signal level also reduces quickly, which limits the observation of thin surface layers.



KBr-overlayer diffuse reflection spectroscopy provides enhanced intensity from sub-micrometer range (17). Figure 5 shows the signal intensity of a two layer polymer film where

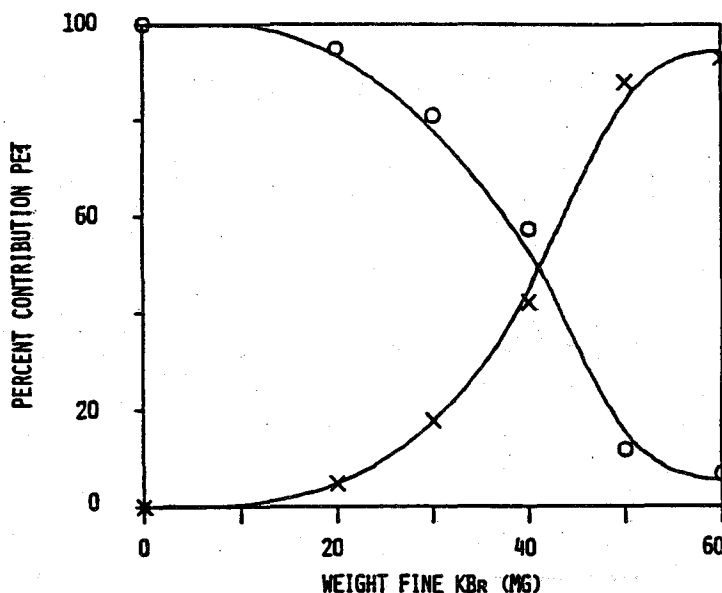


Figure 5. Percent contribution of the 29.5  $\mu\text{m}$ -thick poly (ethylene terephthalate) substrate (○) and the 1.5  $\mu\text{m}$ -thick poly (vinylidene fluoride) overlayer (×) to the composite spectra in the CH stretching region as a function of the weight of the fine (75  $\mu\text{m}$ ) KBr overlayer.

1.5  $\mu\text{m}$  thick poly (vinylidene fluoride) (PVF<sub>2</sub>) is placed on top of a 29.5  $\mu\text{m}$ -thick poly (ethylene terephthalate) (PET). The two-layer polymer film was placed in a diffuse reflectance cell and various amounts of KBr powder were placed on the polymer film. The intensity contribution of the top thin film as compared with the substrate PET increased as the amount of the KBr powder increased, indicating that the surface selectivity increased. It is important to use the KBr powder with the same particle size distribution as the probing depth is influenced by the particle size. While no detailed quantitative evaluation of this technique has been reported to date, it is possible to study selectively a surface film of less than 100 nm on a substrate.

Ordinary attenuated total reflection spectroscopy, one of the oldest surface IR techniques, can probe depth information on the micrometer scale. Pioneering works reported by Harrick (2) and others made this one of the most quantitatively understood techniques. For the total reflection experiment the evanescent wave decays in the following manner:

$$E = E_0 e^{-\frac{2\pi z n_1}{\lambda} \sqrt{\sin^2 \theta - \left(\frac{n_2}{n_1}\right)^2}} \quad \text{Eq [4]}$$

where the subscript, 1, refers to the internal reflection element and 2 refers to the film. Usually, the penetration depth,  $d_p$ , is used to describe the 1/e of the initial field strength and is expressed as:

$$d_p = \frac{\lambda}{2\pi n_1 \sqrt{\sin^2 \theta - \left(\frac{n_2}{n_1}\right)^2}} \quad \text{Eq [5]}$$

Depth probed by the ATR technique is a function of the refractive index difference between the prism and the sample, the angle of incidence, and the frequency. Thus combining the use of these parameters, materials with thickness of less than 1.0  $\mu\text{m}$  to several tens micrometers can be studied. It should be emphasized that the spectrum obtained is a cumulative information from the prism/sample interface. Ohta and Iwamoto indicated that 63% of intensity originated from the 0.5 $d_p$  if Ge prism was used (3.4). Thus, it will be increasingly difficult to observe materials with deeper locations.

Similar depth is probed by the Brewster-angle incidence external reflection spectroscopy, but with depth information influenced by different parameters than the ATR technique (14). The dominant parameter in this method is the specific absorptivity of the particular frequency.

To date, the most quantitative and highest spatial resolution is attained by the variable-angle ATR spectroscopy. The concept of the variable-angle ATR spectroscopy was originated by Tompkins (57) and modified by Hirshfeld (58). It was later advanced by Fina and Chen (59) and Shick and Ishida (60). A Brief theoretical background is discussed below. The absorbance,  $A$ , is expressed as:

$$A = 1 - R = \frac{n_2 \alpha}{n_1 \cos \theta} \int_0^t k(z) E^2 dz \quad \text{Eq [6]}$$

where  $E$  is the evanescent wave decays expressed earlier. However, the absorptivity profile, where  $k$  is extinction coefficient, is unknown. Assuming that the specific absorptivity of a material of interest is constant throughout the thickness, the absorptivity profile is proportional to the concentration profile. For relatively weak absorbers,

$$A(\gamma) = \frac{n_2 \alpha}{n_1 \cos \theta} \int_0^\infty k(z) e^{-2\gamma z} dz \quad \text{Eq [7]}$$

where the decay constant,  $\gamma$ , is expressed as,

$$\gamma = \frac{2\pi n_1 \sqrt{\sin^2 \theta - \left(\frac{n_2}{n_1}\right)^2}}{\lambda} = \frac{1}{d_p} \quad \text{Eq [8]}$$

where  $\lambda$  is the wavelength of the infrared light in medium 2. We are interested in determining the concentration profile,  $c(z)$ . Since  $k(z) = L^{-1}\{A(\gamma)\}$ ,

$$c(z) = \alpha' k(z) = \alpha' L^{-1}\{A(\gamma)\} \quad \text{Eq. [9]}$$

where  $L^{-1}$  is the inverse Laplace transform. If a thin film with some absorption is placed a certain distance away from an internal reflection element as shown in Figure 6, then the Laplace transform of this profile is represented analytically by:

$$L\{A(Z)\} = \frac{\alpha'(e^{-t_1 s} - e^{-t_2 s})}{s \cos \theta} \quad \text{Eq. [10]}$$

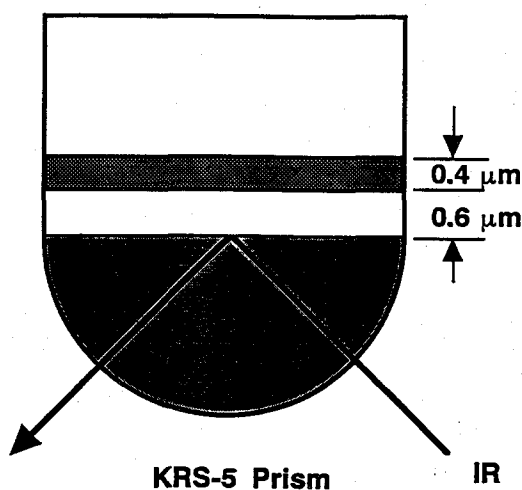


Figure 6. Variable-angle ATR optical configuration of an absorbing thin film placed away from the KRS-5 prism.

where  $s = 2\gamma$ ,  $t_1$  is the thickness of interceding layer, and  $t_2 - t_1$  is the thickness of interesting layer. Then, absorbance,  $A = 1 - R$ , due to this film can be calculated as a function of angle of incidence. The result is shown in Figure 7.

The benefits of this approach are clearly expressed in Figure 8 where it is compared with the traditional method, i.e. as a function of depth of penetration. It is apparent that the traditional approach leads to unrealistic concentration profile while the new approach by fitting the inverse Laplace transform function accurately reproduces the model profile of the stratified layers. It is also possible to specify a layer with a certain thickness and calculate the infrared spectrum of the particular layer. The lower limit of the thickness of the layer depends in part on the accuracy and signal-to-noise ratio of the collected spectrum. At the present time, a layer thickness of a few hundred nanometers is possible, and this spatial resolution will improve with increased understanding of the impact of the assumptions on the intrinsic errors associated with this approach. It should be also mentioned that the optimum range of the range of the sample to be studied depends on the prism material as well as the frequency of the infrared band to be used for the examination.

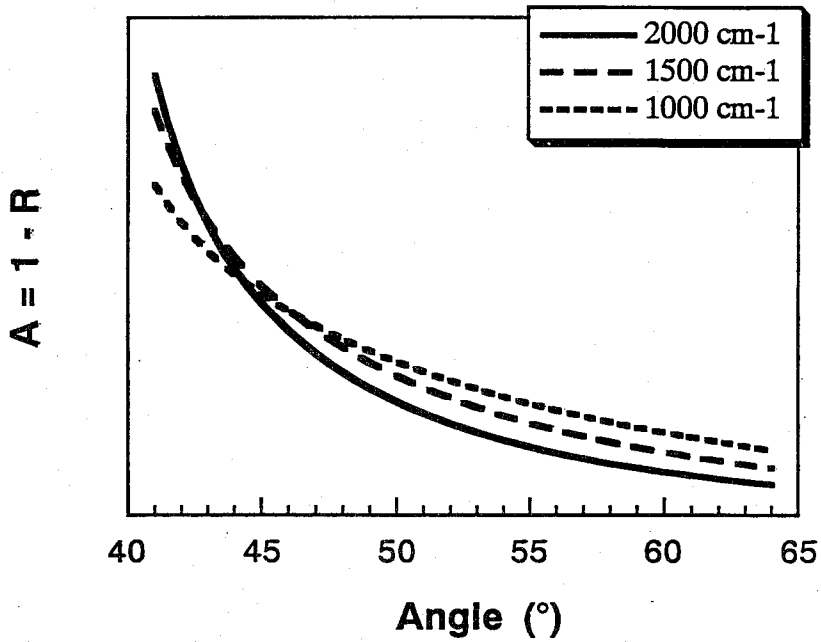


Figure 7. Absorptance,  $A=1-R$ , is plotted as a function of the angle of incidence as well as the frequency.

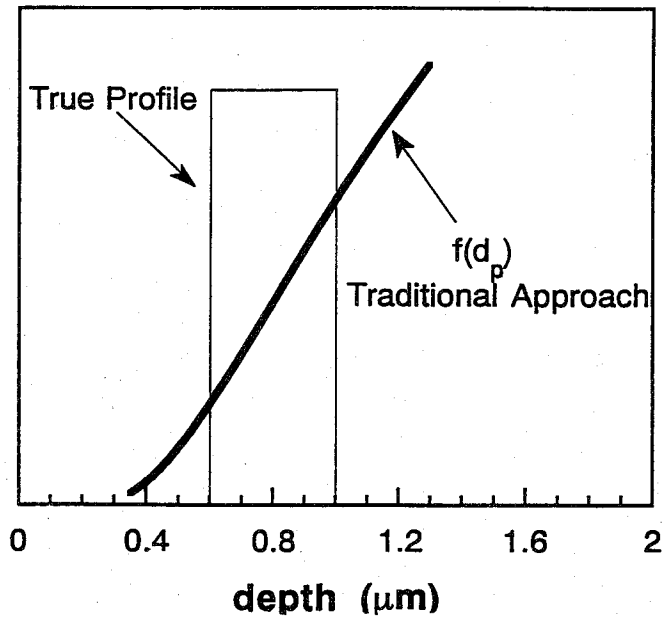


Figure 8. Concentration profile plotted as a function of the depth of penetration showing that the traditional method leads to unrealistic profile. The new approach precisely probes the concentration of the absorbing film shown in Figure 6.

## CONCLUSIONS

With the advancement of computers, application of optical theory to various infrared spectroscopic technique has become a nearly routine operation. Diversified techniques, especially those related to reflection techniques, will show frequency shifts and band shape distortion due to purely optical reasons. Properly applied optical theory programs will identify spectral changes due to the optical reasons and allow the spectrum to be interpreted from a structural point of view. Of particular interest in the progress of quantitative infrared spectroscopy is molecular depth profiling. A significant progress has been made to probe concentration profile of a thin film to less than a few hundred nanometer spatial resolution.

## ACKNOWLEDGMENT

This work was in part supported by the grant from the Office of Naval Research.

## REFERENCES

- (1) A. Taboudoucht and H. Ishida, *Appl. Spectrosc.*, **43**, 1016 (1989).
- (2) N.J. Harrick, "Internal Reflection Spectroscopy," Harrick Scientific, New York (1967).
- (3) R. Iwamoto and K. Ohta, *Appl. Spectrosc.*, **38**, 359 (1984).
- (4) K. Ohta and R. Iwamoto, *Appl. Spectrosc.*, **39**, 418 (1985).
- (5) Y. Ishino and H. Ishida, *Appl. Spectrosc.*, **42**, 1296 (1988).
- (6) H.G. Tompkins, *Appl. Spectrosc.*, **28**, 335 (1974).
- (7) T. Hirschfeld, *Appl. Spectrosc.*, **31**, 289 (1977).
- (8) L. Fina and G. Chen, *Vibrational Spectrosc.*, **1**, 353, (1991).
- (9) R. Shick, J.L. Koenig and H. Ishida, *Appl. Spectrosc.* (submitted).
- (10) S.A. Francis and A.H. Ellison, *J. Opt. Soc. Am.*, **49**, 131 (1959).
- (11) R.G. Greenler, *J. Chem. Phys.*, **44**, 310 (1966).
- (12) D.L. Allara and R.G. Nuzzo, *Langmuir*, **1**, 45, (1985).
- (13) H. Ishida, Y. Ishino, H. Buijs, C. Tripp and M.J. Dignam, *Appl. Spectrosc.*, **41**, 1288 (1987).
- (14) Y. Ishino and H. Ishida, *Appl. Spectrosc.*, (in press)
- (15) M.P. Fuller and P.R. Griffiths, *Anal. Chem.*, **50**, 1906 (1978).
- (16) R.T. Graf, J.L. Koenig and H. Ishida, *Anal. Chem.*, **56**, 773 (1984).
- (17) S.R. Culler, M.T. McKenzie, L.J. Fina, H. Ishida and J.L. Koenig, *Appl. Spectrosc.*, **38**, 791 (1984).
- (18) E.G. Chatzi, H. Ishida and J.L. Koenig, *Appl. Spectrosc.*, **40**, 847 (1986).
- (19) G.N. Zhizhin, M.A. Moskalova, A.A. Sigarev and V.A. Yakovlev, *Opt. Commun.*, **43**, 31 (1982).
- (20) A. Hatta, Y. Chiba and W. Suetaka, *Surf. Sci.*, **158**, 616 (1985).
- (21) Y. Ishino, R.T. Graf and H. Ishida, *Anal. Chem.*, **58**, 2448 (1986).
- (22) Y. Ishino and H. Ishida, *Surface Sci.*, **230**, 299 (1990).
- (23) M.J. Dignam and M.D. Baker, *J. Vac. Sci. Technol.*, **21**, 80 (1982).
- (24) A. Roseler and W. Molgedey, *Infrared Phys.*, **24**, 1 (1984).
- (25) R.T. Graf, J.L. Koenig and H. Ishida, *Anal. Chem.*, **58**, 64 (1986).
- (26) R.T. Graf, J.L. Koenig and H. Ishida, *Appl. Spectrosc.*, **40**, 498 (1986).
- (27) R.G. Greenler, *Surf. Sci.*, **69**, 649 (1977).
- (28) D.L. Allara, D. Teicher and J.F. Durana, *Chem. Phys. Lett.*, **84**, 20 (1981).
- (29) T. Wagatsuma, K. Monma and W. Suetaka, *Appl. Surf. Sci.*, **7**, 281 (1981).
- (30) A. Rosenwaig and A. Gersho, *J. Appl. Phys.*, **47**, 64 (1976).
- (31) Y.C. Teng and B.S.H. Royce, *Appl. Opt.*, **21**, 77 (1982).

- (32) B.S.H. Royce, Y.C. Teng and J.B. Enns, *Ultrason. Symp. Proc.*, 652(1980).
- (33) S.M. Riseman, F.W. Massoth, G.M. Dhar and E.M. Eyring, *J. Phys. Chem.*, **86**, 1760(1982).
- (34) A.C. Boccarra, D. Fournier and J. Badoz, *Appl. Phys. Lett.*, **36**, 130(1980).
- (35) C. Morterra and M.J.D. Low, *Spectrosc. Lett.*, **15**, 689(1982).
- (36) M.J.D. Low and G.A. Parodi, *Spectrosc. Lett.*, **11**, 581(1978).
- (37) H. Ishida, *Rubber Chem. Technol.*, **60**, 497(1987).
- (38) R.T. Graf, J.L. Koenig and H. Ishida in "FT-IR Characterization of Polymers." H. Ishida, Ed., Plenum, New York (1987) p.385.
- (39) J.P. Hawranek and R.N. Jones, *Spectrochim Acta*, **32A**, 111(1976).
- (40) D.L. Allara, A. Baca and C.A. Pryde, *Macromolecules*, **11**, 1215(1978).
- (41) R.T. Graf, J.L. Koenig and H. Ishida, *Appl. Spectrosc.*, **39**, 405(1985).
- (42) T.G. Goplen, D.G. Cameron and R.N. Jones, *Appl. Spectrosc.*, **34**, 657(1980).
- (43) J.E. Bertie and H.H. Eysel, *Appl. Spectrosc.*, **39**, 392(1985).
- (44) J.A. Bardwell and M.J. Dignam, *Anal. Chim. Acta*, **181**, 253(1986).
- (45) M.J. Dignam and S. Mamiche-Afra, *Spectrochim. Acta*, **44A**, 1435(1988).
- (46) K. Ohta and H. Ishida, "Proc. Int. Conf. Fourier Transform Spectroscopy, Sept. 1991."
- (47) A.H. Kachare and W.G. Spitzev, *J. Appl. Phys.*, **45**, 2938(1974).
- (48) J.A. Bardwell and M.J. Dignam, *Anal. Chim. Acta*, **172**, 101(1985).
- (49) B. Harbecke, *Appl. Phys.*, **A40**, 151(1986).
- (50) A. Masui and K. Yamamoto, to be submitted.
- (51) Y. Ishino and H. Ishida, *Appl. Spectrosc.*, **46**, 504(1992).
- (52) R.T. Graf, J.L. Koenig and H. Ishida in "FT-IR Characterization of Polymer." H. Ishida, Ed., Plenum, New York (1987) p.397.
- (53) Y. Ishino and H. Ishida, *Langmuir*, **4**, 846(1988).
- (54) K. Ohta, R.T. Graf and H. Ishida, *Appl. Spectrosc.*, **42**, 114(1988).
- (55) K. Ohta and H. Ishida, *Appl. Opt.*, **29**, 1952(1990).
- (56) K. Ohta and H. Ishida, *Appl. Opt.*, **29**, 2466(1990).
- (57) H.G. Tompkins, *Appl. Spectrosc.*, **28**, 335(1974).
- (58) T. Hirschfeld, *Appl. Spectrosc.*, **31**, 289(1977).
- (59) L. Fina and G. Chen, *Vibrational Spectrosc.*, **1**, 353(1991).
- (60) M. Harada, T. Kitamori, N. Teramae, K. Hashimoto, S. Oda and T. Sawada, *Appl. Spectrosc.*, **46**, 529(1992).
- (61) R. Shick, J.L. Koenig and H. Ishida, *Appl. Spectrosc.* (accepted).